JOURNAL OF GUIDANCE, CONTROL, AND DYNAMICS
Vol. 40, No. 2, February 2017

Engineering Notes

Approximate Closed-Form Solution to a Linear Quadratic Optimal Control Problem with Disturbance

Robert A. E. Zidek* and Ilya V. Kolmanovsky*
University of Michigan, Ann Arbor, Michigan 48109

DOI: 10.2514/1.G001666

I. Introduction

We consider a linear quadratic (LQ) optimal control problem for a class of linear time-invariant systems of the form

$$\dot{x}(t) = Ax(t) + Bu(t) + d(t), \;\; x(0) = x_0 \tag{1}$$

where A and B are real matrices, $x(t) \in \mathbb{R}^n$, $u(t) \in \mathbb{R}^m$, and $d(t) \in \mathbb{R}^n$ is a time-varying disturbance term that is known in advance. Given an initial state x_0, the objective is to find a control u over the finite time horizon $[0, T]$ that minimizes a quadratic cost functional

$$J = \frac{1}{2}\int_0^T [x^T(t)Qx(t) + u^T(t)Ru(t)]\,\mathrm{d}t + \frac{1}{2}x^T(T)Sx(T) \tag{2}$$

with $Q = Q^T \succeq 0$ and $R = R^T \succ 0$. For notational convenience, we may omit indication of the explicit time dependence of time-dependent variables when it is clear from the context.

Problems (1) and (2) are relevant to many real-time optimal control applications: in particular, those where a preview is available or needs to be incorporated [1–5]. According to [6], most prior applications in preview control used discrete-time-based formulations and either H_∞ or linear quadratic regulator (LQR) methods [2,3,7–10]. In contrast, treating the problem in continuous-time (i.e., without resorting to discrete-time approximations) can provide higher solution accuracy. In the continuous-time formulation, optimal control problems (1) and (2) lead to a two-point boundary value problem (TPBVP) with mixed boundary conditions. A solution to this problem is based on solving the Riccati differential equation. In addition, an ordinary differential equation (ODE) that accounts for the disturbance has to be solved [11,12]. In general, there is no explicit solution to this ODE, and numerical and approximate approaches need to be developed. Numerical approaches to solve this ODE are based on integrating backward in time, which may become computationally impractical, especially when larger time horizons are considered.

Therefore, we solve the problem by approximating the disturbance term d as a piecewise-linear function of time. Using Pontryagin's maximum principle, linear systems theory, and analytical integration, we obtain a closed-form solution to the TPBVP. In addition, we derive an upper bound on the error between the optimal solution and the approximate solution when the piecewise-linear disturbance approximation is used. To the best of our knowledge, there has not been a closed-form solution to LQ optimal control problems with previewed disturbance d based on piecewise-linear approximation of d previously established or analyzed/investigated at a level of detail as in this Note. Such an approximation yields higher accuracy than piecewise-constant disturbance approximation that is common in sampled data/discrete-time treatments of the problem.

The presented approach allows fast computation of the optimal control, which facilitates potential onboard/real-time implementation. In particular, this may be useful in applications of model predictive control (MPC) with previewed disturbance [13–16] or with disturbance scenarios [17], where an LQ problem with a disturbance term similar to Eqs. (1) and (2) has to be solved repeatedly over a receding time horizon. Future research to address the inclusion of constraints can further extend the use of our techniques for MPC with a preview to constrained problems.

As our subsequent example demonstrates (Sec. IV), the proposed strategy can be effective in spacecraft orbital maneuvering problems to account for higher-order gravity perturbations and air drag. We note that, in this example, the disturbance is computed for the trajectory of the nominal/target orbit. Because, in the example, the spacecraft is relatively close to the known target orbit, the error is small and the simulation results show that our proposed approach is effective in the context of controlling a nonlinear system: in particular, when recomputing the control over a receding time horizon using MPC techniques to account for unmodeled effects (Sec. IV.C). At the same time, given that the focus of our theoretical analysis is an LQ problem with previewed disturbance, we also include simulation results for the linear model in Sec. IV.B because they illustrate the conclusions from the analysis in a setting consistent with the assumptions in this Note.

The developments in this Note are further motivated by enhancing the implementation of a computational strategy to solve nonlinear optimal control problems, where one iterates between using d to approximate a nonlinear term $d^{i+1} = \phi(x^i)$ in the equations of motion evaluated on a current iteration i of the trajectory and solving the optimal control problem given by Eqs. (1) and (2) [18].

The structure of this Note is as follows. In Sec. II, the necessary conditions for optimality are presented and the closed-form solution to the TPBVP is derived. Section III includes an analysis of the error incurred by the piecewise-linear approximation of d. The method is demonstrated for orbital maneuvering in Sec. IV. Section V provides a conclusion of the work.

II. Solution to the TPBVP

The necessary conditions for optimality in problems (1) and (2) are provided by Pontryagin's maximum principle applied to the Hamiltonian H:

$$H = \frac{1}{2}[x^T Qx + u^T Ru] + \psi^T[Ax + Bu + d] \tag{3}$$

The optimal control minimizes the Hamiltonian. Hence, $u = -R^{-1}B^T\psi$, where ψ denotes the vector of adjoint variables, which satisfy

$$\dot{\psi} = -(\partial H/\partial x)^T = -Qx - A^T\psi \tag{4}$$

Moreover, the transversality condition $\psi(T) = Sx(T)$ must be satisfied. Consequently, we obtain

Received 31 August 2015; revision received 23 October 2016; accepted for publication 24 November 2016; published online 30 January 2017.

*Department of Aerospace Engineering.

$$\begin{bmatrix} \dot{x} \\ \dot{\psi} \end{bmatrix} = \begin{bmatrix} A & -BR^{-1}B^T \\ -Q & -A^T \end{bmatrix} \begin{bmatrix} x \\ \psi \end{bmatrix} + \begin{bmatrix} d \\ 0_{n\times 1} \end{bmatrix} \tag{5}$$

By defining $\tilde{x}^T = [x^T, \psi^T]$ and $\tilde{d}^T = [d^T, 0_{1\times n}]$, Eq. (5) may be written as

$$\dot{\tilde{x}} = \tilde{A}\,\tilde{x} + \tilde{d} \tag{6}$$

with initial condition $\tilde{x}_0^T = \tilde{x}^T(0) = [x_0^T, \psi_0^T]$, where ψ_0 is unknown. Using the transversality condition for ψ, the terminal state values at time T are $\tilde{x}^T(T) = [x^T(T), (Sx(T))^T]$, where $x(T)$ is unknown. However, $x(T)$ or $\tilde{x}(T)$, respectively, can be computed according to

$$\tilde{x}(T) = \mathrm{e}^{\tilde{A}T}\tilde{x}_0 + \int_0^T \mathrm{e}^{\tilde{A}(T-\tau)}\tilde{d}(\tau)\,\mathrm{d}\tau \tag{7}$$

The key assumption for deriving a closed-form approximate solution to the TPBVP is that the disturbance d is approximated by a piecewise-linear function of time. We consider

$$(\nu-1)\text{-equidistant time intervals of length } \Delta t$$

and $t_k = (k-1)\Delta t$, $k = 1, 2, \ldots, \nu$, where the final time is $t_\nu = T = (\nu-1)\Delta t$ and t_1 is at $t = 0$. In analogy, we define $\tilde{d}_k = \tilde{d}(t_k)$. Then, the piecewise-linear approximation (such an approximation can also be referred to as piecewise affine, which is actually more correct) of the disturbance vector $\tilde{d}(t)$ at time t is given by

$$\tilde{d}_{\mathrm{pwlin}}(t) = \tilde{d}_k + \frac{\tilde{d}_{k+1} - \tilde{d}_k}{\Delta t}(t - (k-1)\Delta t), \text{ for } t \in [t_k, t_{k+1}] \tag{8}$$

Consequently, the approximation of Eq. (7) using Eq. (8) is

$$\tilde{x}_{\mathrm{pwlin}}(T) = \mathrm{e}^{\tilde{A}T}\tilde{x}_0 + \sum_{k=1}^{\nu-1}\left\{\int_{(k-1)\Delta t}^{k\Delta t} \mathrm{e}^{\tilde{A}(T-\tau)} \times \left[\tilde{d}_k + \frac{\tilde{d}_{k+1} - \tilde{d}_k}{\Delta t}(\tau - (k-1)\Delta t)\right]\mathrm{d}\tau\right\} \tag{9}$$

A. Case $\tilde{A}$ Is Invertible

When $\tilde{A}$ is nonsingular, integration by parts of Eq. (9) and further simplification yields

$$\tilde{x}_{\mathrm{pwlin}}(T) = \mathrm{e}^{\tilde{A}T}\tilde{x}_0 + \tilde{A}^{-1}\sum_{k=1}^{\nu-1}\left\{\mathrm{e}^{\tilde{A}(\nu-k)\Delta t}\tilde{d}_k - \mathrm{e}^{\tilde{A}(\nu-k-1)\Delta t}\tilde{d}_{k+1} + \tilde{A}^{-1}\left(\mathrm{e}^{\tilde{A}(\nu-k)\Delta t} - \mathrm{e}^{\tilde{A}(\nu-k-1)\Delta t}\right)\left(\frac{\tilde{d}_{k+1} - \tilde{d}_k}{\Delta t}\right)\right\} \tag{10}$$

We introduce the constant matrices $K_k \in \mathbb{R}^{2n\times 2n}$ defined by

$$K_k = \mathrm{e}^{\tilde{A}(k-1)\Delta t}, \qquad k = 1, 2, \ldots, \nu \tag{11}$$

and Eq. (10) is rewritten as

$$\tilde{x}_{\mathrm{pwlin}}(T) = K_\nu\tilde{x}_0 + \tilde{A}^{-1}(K_\nu\tilde{d}_1 - K_1\tilde{d}_\nu) + (\tilde{A}^{-1})^2\sum_{k=1}^{\nu-1}\left\{(K_{\nu+1-k} - K_{\nu-k})\left(\frac{\tilde{d}_{k+1} - \tilde{d}_k}{\Delta t}\right)\right\} \tag{12}$$

which provides $2n$ equations to solve for the $2n$ unknowns contained in ψ_0 and $x(T)$. To solve the system of linear equations, the sum of the second and third terms in Eq. (12) is denoted by $q^T = [q_1^T, q_2^T]$,

$$q = \tilde{A}^{-1}(K_\nu\tilde{d}_1 - K_1\tilde{d}_\nu) + (\tilde{A}^{-1})^2\sum_{k=1}^{\nu-1}\left\{(K_{\nu+1-k} - K_{\nu-k})\left(\frac{\tilde{d}_{k+1} - \tilde{d}_k}{\Delta t}\right)\right\} \tag{13}$$

where $q_1, q_2 \in \mathbb{R}^{n\times 1}$. Then, it follows that

$$\tilde{x}_{\mathrm{pwlin}}(T) = \begin{bmatrix} x_{\mathrm{pwlin}}(T) \\ Sx_{\mathrm{pwlin}}(T) \end{bmatrix} = K_\nu\begin{bmatrix} x_0 \\ \psi_{0,\mathrm{pwlin}} \end{bmatrix} + q \tag{14}$$

where $x_{\mathrm{pwlin}}(T)$ and $\psi_{0,\mathrm{pwlin}}$ are the approximations of $x(T)$ and ψ_0 using the piecewise-linear disturbance term. By noting that

$$K_\nu = \begin{bmatrix} K_{\nu,11} & K_{\nu,12} \\ K_{\nu,21} & K_{\nu,22} \end{bmatrix}$$

and $K_{\nu,ij} \in \mathbb{R}^{n\times n}$, the solution to the TPBVP is given by

$$\begin{bmatrix} x_{\mathrm{pwlin}}(T) \\ \psi_{0,\mathrm{pwlin}} \end{bmatrix} = \begin{bmatrix} I_{n\times n} - K_{\nu,12}C_{\mathrm{inv}}S & K_{\nu,12}C_{\mathrm{inv}} \\ -C_{\mathrm{inv}}S & C_{\mathrm{inv}} \end{bmatrix}\begin{bmatrix} K_{\nu,11}x_0 + q_1 \\ K_{\nu,21}x_0 + q_2 \end{bmatrix} \tag{15}$$

where $C_{\mathrm{inv}} = (SK_{\nu,12} - K_{\nu,22})^{-1}$. Now, by following the same steps and noting that $x_0 = x_{0,\mathrm{pwlin}}$, we can derive the solution to the state equation that, at the discrete time steps t_k, reads

$$\tilde{x}_{\mathrm{pwlin}}(t_k) = K_k\tilde{x}_{0,\mathrm{pwlin}} + \tilde{A}^{-1}(K_k\tilde{d}_1 - K_1\tilde{d}_k) + (\tilde{A}^{-1})^2\sum_{i=1}^{k-1}\left\{(K_{k+1-i} - K_{k-i})\left(\frac{\tilde{d}_{i+1} - \tilde{d}_i}{\Delta t}\right)\right\} \tag{16}$$

and the approximate optimal control at the kth time instant is

$$u_{\mathrm{pwlin}}(t_k) = -R^{-1}B^T[0_{n\times n}, I_{n\times n}]\tilde{x}_{\mathrm{pwlin}}(t_k) \tag{17}$$

B. Case $\tilde{A}$ Is Not Invertible

When $\tilde{A}$ is not invertible, it has $p \in \{0, 1, \ldots, 2n-1\}$ nonzero eigenvalues and there exists an invertible matrix $M \in \mathbb{C}^{2n\times 2n}$ such that $\tilde{A}$ can be decomposed as

$$\tilde{A} = M\begin{bmatrix} J_1 & 0_{p\times(2n-p)} \\ 0_{(2n-p)\times p} & J_2 \end{bmatrix}M^{-1} \tag{18}$$

where $J_1 \in \mathbb{C}^{p\times p}$ is invertible, and $J_2 \in \mathbb{R}^{(2n-p)\times(2n-p)}$ is not invertible (see Chap. 6.2 in [19]). Therefore, the integral of the matrix exponential may be written as

$$\int_{t_n}^{t_{n+1}} \mathrm{e}^{\tilde{A}(t_k-\tau)}\,\mathrm{d}\tau = M\begin{bmatrix} -J_1^{-1}(\mathrm{e}^{J_1(t_k-t_{n+1})} - \mathrm{e}^{J_1(t_k-t_n)}) & 0_{p\times(2n-p)} \\ 0_{(2n-p)\times p} & \int_{t_n}^{t_{n+1}} \mathrm{e}^{J_2(t_k-\tau)}\,\mathrm{d}\tau \end{bmatrix}M^{-1} \tag{19}$$

The integral of $\mathrm{e}^{J_2(t_k-\tau)}$ with respect to τ depends on the number (algebraic multiplicity) of zero eigenvalues of $\tilde{A}$ as well as on the dimension of the null space of $\tilde{A}$. A procedure that distinguishes between the possible cases may be implemented for computation purposes; see [19]. To solve the integral of the matrix exponential in Eq. (9), we define the following indefinite integrals or antiderivatives:

$$\int \mathrm{e}^{\tilde{A}(t_k-\tau)}\,\mathrm{d}\tau = F_k(\tau) + C, \qquad \int F_k(\tau)\,\mathrm{d}\tau = G_k(\tau) + C \tag{20}$$

where $C \in \mathbb{R}^{2n\times 2n}$ is a constant matrix, and $F_k(\tau)$ and $G_k(\tau)$ are the respective antiderivatives for a given k and $\tau \in [0, T]$. Note that, in general, the antiderivative $Z(x)$ of a function $z(x)$, $x \in I$, satisfies $\mathrm{d}Z(x)/\mathrm{d}x = z(x)$ for $x \in I$, where

$$\int z(x)\,\mathrm{d}x = Z(x) + C$$

and $C = \text{const}$. With F_k and G_k, integration by parts of Eq. (9) yields

$$\tilde{x}_{\text{pwlin}}(T) = \mathrm{e}^{\tilde{A}T}\tilde{x}_0 + F_\nu(T)\tilde{d}_\nu - F_\nu(0)\tilde{d}_1 + \sum_{k=1}^{\nu-1}\left\{[G_\nu(k\Delta t) - G_\nu((k-1)\Delta t)]\left[\frac{\tilde{d}_{k+1} - \tilde{d}_k}{\Delta t}\right]\right\} \quad (21)$$

Based on Eq. (20), the following constant matrices are defined:

$$\tilde{F}_{i,k} = F_k((i-1)\Delta t),\ \tilde{G}_{i,k} = G_k((i-1)\Delta t) \quad (22)$$

with $i = 1, 2, \ldots, \nu$ and $k = 1, 2, \ldots, \nu$. Using Eqs. (11) and (22), we write Eq. (21) as

$$\tilde{x}_{\text{pwlin}}(T) = K_\nu\tilde{x}_0 + \tilde{F}_{\nu,\nu}\tilde{d}_\nu - \tilde{F}_{1,\nu}\tilde{d}_1 + \sum_{k=1}^{\nu-1}\left\{[\tilde{G}_{k+1,\nu} - \tilde{G}_{k,\nu}]\left[\frac{\tilde{d}_{k+1} - \tilde{d}_k}{\Delta t}\right]\right\} \quad (23)$$

In analogy to Eq. (13), the constant vector $q^T = [q_1^T, q_2^T]$ is defined in order to solve the TPBVP:

$$q = \tilde{F}_{\nu,\nu}\tilde{d}_\nu - \tilde{F}_{1,\nu}\tilde{d}_1 + \sum_{k=1}^{\nu-1}\left\{[\tilde{G}_{k+1,\nu} - \tilde{G}_{k,\nu}]\left[\frac{\tilde{d}_{k+1} - \tilde{d}_k}{\Delta t}\right]\right\} \quad (24)$$

Now, the initial adjoint variables $\psi_{0,\text{pwlin}}$ and the final state vector $x_{\text{pwlin}}(T)$ can be obtained according to Eq. (15). Similarly, we can derive the solution to the state equations at the discrete time steps t_k:

$$\tilde{x}_{\text{pwlin}}(t_k) = K_k\tilde{x}_{0,\text{pwlin}} + \tilde{F}_{k,k}\tilde{d}_k - \tilde{F}_{1,k}\tilde{d}_1 + \sum_{i=1}^{k-1}\left\{(\tilde{G}_{i+1,k} - \tilde{G}_{i,k})\left(\frac{\tilde{d}_{i+1} - \tilde{d}_i}{\Delta t}\right)\right\} \quad (25)$$

and the approximate optimal control is computed according to Eq. (17).

III. Error Estimation

In this section, we derive an upper bound for the error between the optimal solution $\tilde{x}(t)$ and its approximation $\tilde{x}_{\text{pwlin}}(t)$. For the derivation, we make the following assumptions:

Assumption 1: For $t \in [0, T]$, $\tilde{d}(t)$ is twice continuously differentiable.

Assumption 2: The matrices S and $\tilde{A}$ are such that $C_T \exp(\tilde{A}T) = [K_1, K_2]$, where $K_2 \in \mathbb{R}^{n\times n}$ has rank n and $C_T = [S, -I_{n\times n}]$.

Our numerical experiences suggest that Assumption 2 holds. This may be because, for most applications, the diagonal elements of $\exp(\tilde{A}T)$ are nonzero (see infinite power series representation for matrix exponentials [19], where the first term is the identity matrix) and S is usually diagonal. In the following, $\|\cdot\| = \|\cdot\|_p$ denotes the p norm or Hölder norm [19] of a vector or matrix and $\exp(\cdot) = \mathrm{e}^{(\cdot)}$.

Proposition 1: Suppose Assumptions 1 and 2 hold. Then, for $t \in [0, T]$,

$$\|\tilde{x}(t) - \tilde{x}_{\text{pwlin}}(t)\| \le \exp(\|\tilde{A}\|t)\left[\max_{a\in[0,T]}\left\|\ddot{\tilde{d}}(a)\right\|4t\Delta t^2/27 + M(\Delta t^2)\right]$$

where

$$M(\Delta t^2) = \|C_T\|\left\|\begin{bmatrix} C_T\exp(\tilde{A}T) \\ C_0 \end{bmatrix}^{-1}\right\| \times \|\exp(\tilde{A}T)\| \max_{a\in[0,T]}\|\ddot{\tilde{d}}(a)\|4T\Delta t^2/27$$

with $C_0 = [I_{n\times n}, 0_{n\times n}]$ and $C_T = [S, -I_{n\times n}]$.

Proof: First, a bound for $\|\tilde{d}(t) - \tilde{d}_{\text{pwlin}}(t)\|$ is derived. In contrast to the piecewise-linear $\tilde{d}_{\text{pwlin}}(t)$, the continuous $\tilde{d}(t)$ is differentiable at each of the discrete time points t_k, $k = 1, 2, \ldots, \nu$. Using Taylor's theorem, we express $\tilde{d}(t_k)$ and $\tilde{d}(t_{k+1})$ as

$$\tilde{d}(t_k) = \tilde{d}(t) + (t_k - t)\dot{\tilde{d}}(t) + \frac{1}{2}(t_k - t)^2\ddot{\tilde{d}}(a_1),$$
$$\tilde{d}(t_{k+1}) = \tilde{d}(t) + (t_{k+1} - t)\dot{\tilde{d}}(t) + \frac{1}{2}(t_{k+1} - t)^2\ddot{\tilde{d}}(a_2) \quad (26)$$

where $t \in [t_k, t_{k+1}]$, $a_1 \in [t_k, t]$, and $a_2 \in [t, t_{k+1}]$. By noting that $\tilde{d}(t_k) = \tilde{d}_k$ and $\tilde{d}(t_{k+1}) = \tilde{d}_{k+1}$, the expression for $\tilde{d}_{\text{pwlin}}(t)$ in Eq. (8) can be stated as

$$\tilde{d}_{\text{pwlin}}(t) = \frac{t_{k+1} - t}{\Delta t}\tilde{d}(t_k) - \frac{t_k - t}{\Delta t}\tilde{d}(t_{k+1}) \quad (27)$$

Using Eq. (26) and $\Delta t = t_{k+1} - t_k$, Eq. (27) becomes

$$\tilde{d}_{\text{pwlin}}(t) = \tilde{d}(t) + \frac{\ddot{\tilde{d}}(a_1)}{2\Delta t}(t_{k+1} - t)(t_k - t)^2 + \frac{\ddot{\tilde{d}}(a_2)}{2\Delta t}(t - t_k)(t_{k+1} - t)^2 \quad (28)$$

It follows from Eq. (28) that, for $t \in [t_k, t_{k+1}]$, the error between $\tilde{d}(t)$ and $\tilde{d}_{\text{pwlin}}(t)$ is bounded by

$$\|\tilde{d}_{\text{pwlin}}(t) - \tilde{d}(t)\| \le \left\|\frac{\ddot{\tilde{d}}(a_1)}{2\Delta t}(t_{k+1} - t)(t_k - t)^2 + \frac{\ddot{\tilde{d}}(a_2)}{2\Delta t}(t - t_k)(t_{k+1} - t)^2\right\| \le \frac{\|\ddot{\tilde{d}}(a_1)\|}{2\Delta t}(t_{k+1} - t)(t_k - t)^2 + \frac{\|\ddot{\tilde{d}}(a_2)\|}{2\Delta t}(t - t_k)(t_{k+1} - t)^2 \le \frac{2\Delta t^2}{27}(\|\ddot{\tilde{d}}(a_1)\| + \|\ddot{\tilde{d}}(a_2)\|) \le \frac{4\Delta t^2}{27}\max_{a\in[t_k,t_{k+1}]}\|\ddot{\tilde{d}}(a)\| \quad (29)$$

because $(t_{k+1} - t)(t_k - t)^2 \le 4\Delta t^3/27$ and $(t - t_k)(t_{k+1} - t)^2 \le 4\Delta t^3/27$. The error between the solutions to Eq. (6) is denoted by $e(t) = \tilde{x}(t) - \tilde{x}_{\text{pwlin}}(t)$. Using Eq. (6), the time derivative of the error is $\dot{e}(t) = \dot{\tilde{d}}(t) - \dot{\tilde{d}}_{\text{pwlin}}(t) + \tilde{A}e(t)$. Integrating this expression yields

$$e(t) = \int_0^t [\dot{\tilde{d}}(\tau) - \dot{\tilde{d}}_{\text{pwlin}}(\tau) + \tilde{A}e(\tau)]\,\mathrm{d}\tau + e(0) \quad (30)$$

It follows from Eq. (30) and the triangle inequality that

$$\|e(t)\| \le \int_0^t \|\dot{\tilde{d}}(\tau) - \dot{\tilde{d}}_{\text{pwlin}}(\tau)\|\,\mathrm{d}\tau + \int_0^t \|\tilde{A}\|\|e(\tau)\|\,\mathrm{d}\tau + \|e(0)\| \quad (31)$$

Using the Gronwall–Bellman inequality [20], Eq. (31) becomes

$$\|e(t)\| \le \left[\int_0^t \|\dot{\tilde{d}}(\tau) - \dot{\tilde{d}}_{\text{pwlin}}(\tau)\|\,\mathrm{d}\tau + \|e(0)\|\right]\exp(\|\tilde{A}\|t) \quad (32)$$

Next, we derive an error bound for $\|e(0)\|$. Using the transversality condition for the adjoint variables, as well as the fact that the initial error between the states is zero, we obtain the following equations

$$C_T e(T) = 0_{n\times 1} \quad (33)$$

$$C_0 e(0) = 0_{n\times 1} \quad (34)$$

where $C_T = [S, -I_{n\times n}]$ and $C_0 = [I_{n\times n}, 0_{n\times n}]$. Using Eq. (30), Eq. (33) may be expressed as

$$C_T \exp(\tilde{A}T)e(0) + C_T \int_0^T \exp(\tilde{A}(T-\tau)) \times (\tilde{d}(\tau) - \tilde{d}_{\text{pwlin}}(\tau))\,\mathrm{d}\tau = 0_{n\times 1} \tag{35}$$

Combining Eqs. (34) and (35) yields

$$e(0) = \begin{bmatrix} C_T \exp(\tilde{A}T) \\ C_0 \end{bmatrix}^{-1} \times \begin{bmatrix} -C_T \int_0^T \exp(\tilde{A}(T-\tau))(\tilde{d}(\tau) - \tilde{d}_{\text{pwlin}}(\tau))\,\mathrm{d}\tau \\ 0_{n\times 1} \end{bmatrix} \tag{36}$$

where the inverse exists by Assumption 2. Finally, Eq. (36) implies that

$$\|e(0)\| \le \|C_T\| \left\| \begin{bmatrix} C_T \exp(\tilde{A}T) \\ C_0 \end{bmatrix}^{-1} \right\| \times \sum_{k=1}^{T/\Delta t} \left\{ \int_{t_k}^{t_{k+1}} \|\exp(\tilde{A}(T-\tau))(\tilde{d}(\tau) - \tilde{d}_{\text{pwlin}}(\tau))\|\,\mathrm{d}\tau \right\} \tag{37}$$

Using Eqs. (29) and (37), we obtain

$$\|e(0)\| \le \|C_T\| \left\| \begin{bmatrix} C_T \exp(\tilde{A}T) \\ C_0 \end{bmatrix}^{-1} \right\| \max_{\tau\in[0,T]} \|\exp(\tilde{A}(T-\tau))\| \times \frac{T}{\Delta t} \frac{4\Delta t^3}{27} \max_{a\in[0,T]} \|\ddot{\tilde{d}}(a)\| \le \|C_T\| \left\| \begin{bmatrix} C_T \exp(\tilde{A}T) \\ C_0 \end{bmatrix}^{-1} \right\| \times \left\| \exp(\tilde{A}T) \right\| \frac{4T\Delta t^2}{27} \max_{a\in[0,T]} \left\| \ddot{\tilde{d}}(a) \right\| \tag{38}$$

For notational convenience we denote the error bound for $e(0)$ by M, which is a function of Δt^2:

$$M(\Delta t^2) = \|C_T\| \left\| \begin{bmatrix} C_T \exp(\tilde{A}T) \\ C_0 \end{bmatrix}^{-1} \right\| \times \left\| \exp(\tilde{A}T) \right\| \frac{4T\Delta t^2}{27} \max_{a\in[0,T]} \left\| \ddot{\tilde{d}}(a) \right\| \tag{39}$$

With Eqs. (38) and (39), the error bound for $e(t)$ in Eq. (32) may be stated as

$$\|e(t)\| \le \left[t \frac{4\Delta t^2}{27} \max_{a\in[0,T]} \left\| \ddot{\tilde{d}}(a) \right\| + M(\Delta t^2) \right] \exp(\|\tilde{A}\| t) \tag{40}$$

IV. Example: Spacecraft Orbital Maneuver

In this section, the proposed method is used for spacecraft orbital maneuvering. The control problem, including the nonlinear and linearized spacecraft models, is described in Sec. IV.A. Section IV.B presents the open-loop solution based on the linear model and numerically quantifies the error incurred by the piecewise-linear approximation of the disturbance. Then, in Sec. IV.C, a receding horizon control (RHC) implementation of the linear-model-based controller is applied to the nonlinear model. All computations in this section were performed in MATLAB 2015a on a laptop with an i5-6300 processor.

A. Control Problem

We consider the following nonlinear equations of motion:

$$\ddot{r} = -\frac{\mu}{\|r\|_2^3} r - \frac{1}{2BC} \rho \|\dot{r}\|_2 \dot{r} + f_g + u \tag{41}$$

where r is the position vector of the spacecraft relative to the center of the attracting body, u denotes the vector of control input accelerations, and μ is the gravitational parameter associated with the two-body problem. The second term in Eq. (41) represents the perturbation due to atmospheric drag, where BC is the spacecraft's ballistic coefficient and ρ is the density of the atmosphere, which is computed using the NRLMSISE-00 model [21]. In this model, we neglect the effect of a moving atmosphere. The third term f_g in Eq. (41) is a nonlinear function of r, representing the J_2 and J_3 perturbations (see [22]) that, in addition to atmospheric drag, are the major perturbations for low Earth orbits. In general, our approach allows us to consider any kind of disturbances, and additional perturbations can be readily included.

An optimal control problem with the cost functional [Eq. (2)] is considered, where the quadratic penalty on the control u reflects propellant consumption for a variable specific impulse (VSI) thruster [23]. The linear model is obtained by linearizing the nonlinear model in Eq. (41) around a circular target/desired orbit and is given by the Clohessy–Wiltshire (CW) equations; see [24]. The CW equations describe the spacecraft's motion in the Hill's frame, where the x axis is along the radial direction and the z axis is orthogonal to the orbital plane of the nominal orbit (pointing in the direction of the nominal orbit's angular momentum vector). The y axis completes the right-hand frame and is along the velocity vector of the nominal orbit. The state vector in the Hill's frame is $x^T = [r_x, r_y, r_z, v_x, v_y, v_z]$, describing the position and velocity of the spacecraft relative to the target orbit. The control vector is $u^T = [u_x, u_y, u_z]$, where u_x, u_y, and u_z are accelerations in the respective directions of the Hill's frame. The time-varying disturbance term as viewed from the Hill's frame is $d^T = [0, 0, 0, d_x, d_y, d_z]$. It is obtained by calculating the respective disturbances (i.e., $-0.5\rho_0\|\dot{r}_0\|_2\dot{r}_0/BC + f_{g,0}$) for the known nominal orbit, and then transforming the vectors from the Earth-centered inertial (ECI) frame to the Hill's frame.

A generic spacecraft with a mass of $m = 250$ kg is considered. For the linear model, we only take into account atmospheric drag along the nominal orbital track direction (y direction), where a relevant surface area of $A = 5$ m^2 and a drag coefficient of 2.5 are assumed, yielding a ballistic coefficient of $BC = 20$ kg/m^2. The weights for the cost function are chosen as $Q = 0_{6\times 6}$, $R = \text{diag}(10, 10, 10)$, and $S = \text{diag}(10^6, 10, 10^6, 10^6, 10^6, 10^6)$, emphasizing achievement of the desired final state [except for the final position $r_y(T)$ on the target orbit] with minimum propellant consumption with a VSI low-thrust engine. The emphasis on minimum fuel consumption may be increased by either lowering the diagonal elements of S or increasing the diagonal elements of R, which may, however, increase the error in the final state. Note that the approach does not take into account hard constraints on the state and control inputs. However, matrices Q, R, and S provide tuning parameters by which maximum state and control deviators can be affected. Moreover, in some problems, nearly feasible solutions are acceptable, especially when no strictly feasible solution exists.

Two different cases with different target orbits and initial conditions are considered. In each case, we set the maneuver time T to the orbital period of the nominal orbit. The first case assumes a target orbit altitude of 250 km with an inclination of $i = 30$ deg; a right ascension of the ascending node (RAAN) of 50 deg; and an orbital period $T = 1.49$ h, where the initial condition is given by $r_x(0) = r_y(0) = 20$ km and $r_z(0) = v_x(0) = v_y(0) = v_z(0) = 0$. The second case assumes a 1000 km target orbit with $i = -50$ deg; RAAN $= 0$; and an orbital period of $T = 1.75$ h, where $r_x(0) = -100$ km, $r_y(0) = 60$ km, $r_z(0) = 40$ km, $v_x(0) = -80$ m/s, $v_y(0) = 10$ m/s, and $v_z(0) = 40$ m/s.

B. Linear Model Results

The results for the linear model [Eq. (1)] are analyzed in this subsection. Figure 1 (top) shows the time history of the relative control input error $u_{\text{rel}}(t) = \|u(t) - u_{\text{pwlin}}(t)\|/\|u(t)\|$ for the two test cases using a sampling time of $\Delta t = t_{k+1} - t_k = 100$ s, where u is the optimal solution when the actual d rather than its approximation is used. Moreover, the average error

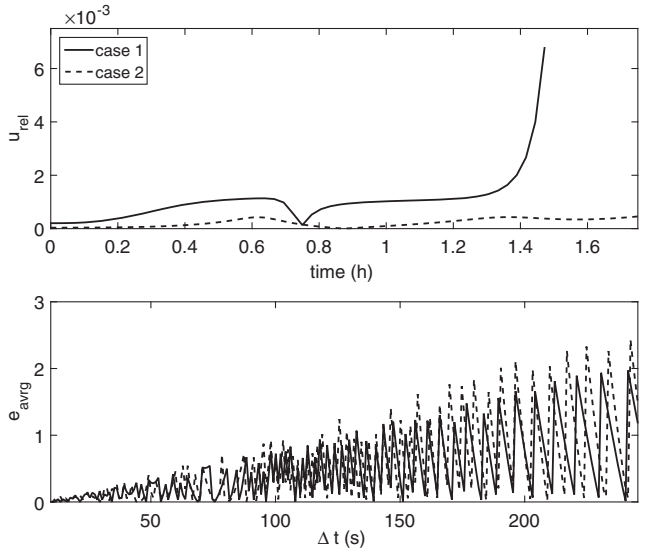

Fig. 1 Linear model results: relative control input error $u_{\mathrm{rel}}(t) = \|u(t) - u_{\mathrm{pwlin}}(t)\|/\|u(t)\|$ for $\Delta t = 100$ s (top), and average error $e_{\mathrm{avrg}} = \sum_{k=1}^{\nu} \|\tilde{x}(t_k) - \tilde{x}_{\mathrm{pwlin}}(t_k)\|/\nu$ vs sampling time Δt (bottom).

$$e_{\mathrm{avrg}} = \sum_{k=1}^{\nu} \|\tilde{x}(t_k) - \tilde{x}_{\mathrm{pwlin}}(t_k)\|/\nu$$

of the augmented state vector is plotted against Δt in the bottom of Fig. 1. Note that, throughout this section, we use the 2-norm and units of kilometers and seconds to compute cost values and norms. The relative control input error incurred by the piecewise-linear approximation of d with $\Delta t = 100$ s is less than 0.1% for most of the maneuver time and never exceeds 0.8% according to Fig. 1. Furthermore, in line with Proposition 1, the average error e_{avrg} can be bounded by a quadratic function of Δt.

Figure 2 shows the required computation times for our proposed method for different sampling times Δt. The total computation time is the sum of the required time to build the matrices in Eqs. (11) and (20) (top plot in Fig. 2), the time to solve the TPBVP (i.e., obtain $\psi_{0,\mathrm{pwlin}}$) (middle plot), and the time to compute the state and control sequences for all t_k (bottom plot). In general, the computation times are decreasing exponentially with increasing Δt, and the major part of the total computation time is due to building the matrices (top plot in Fig. 2). For practical applications, this needs to be done only once and can be performed offline. Solving the TPBVP and obtaining the state

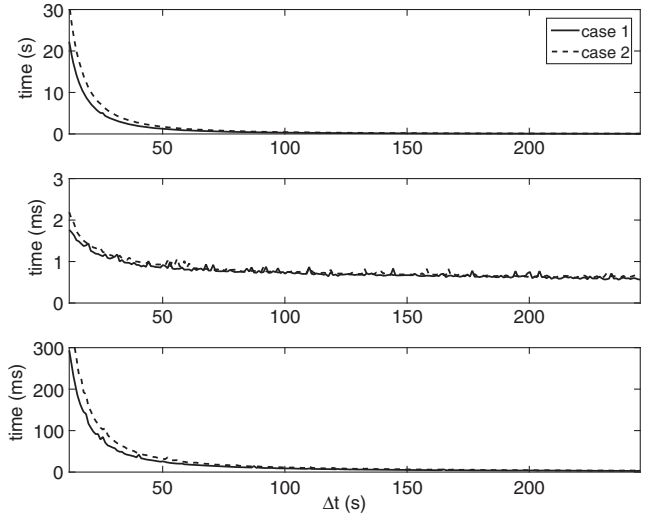

Fig. 2 Computation times vs Δt: time to build the matrices in Eqs. (11) and (20) (top), time to solve the TPBVP (middle), and time to compute $\tilde{x}_{\mathrm{pwlin}}(t)$ and $u_{\mathrm{pwlin}}(t)$ for all t_k (bottom).

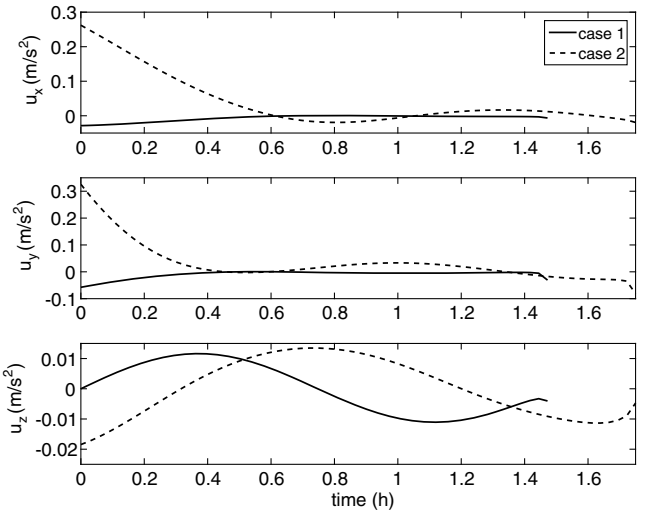

Fig. 3 Nonlinear model results with RHC: control input acceleration in Hill's frame vs time.

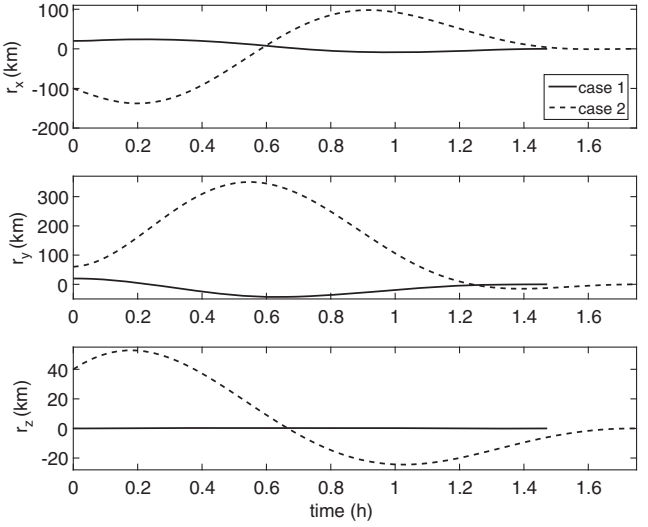

Fig. 4 Nonlinear model results with RHC: spacecraft position in Hill's frame vs time.

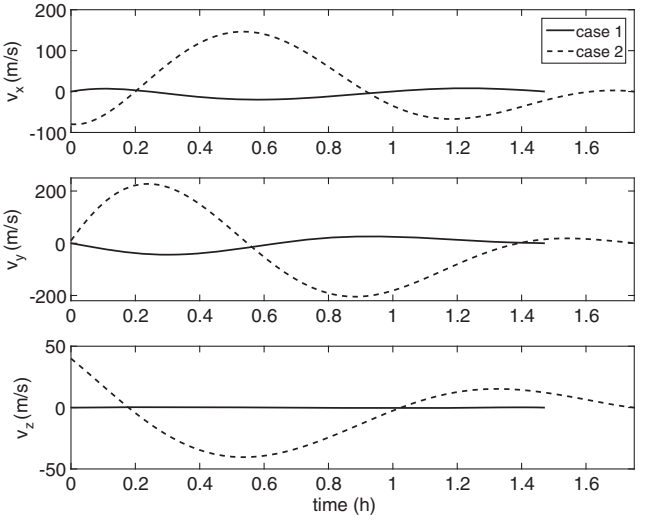

Fig. 5 Nonlinear model results with RHC: spacecraft velocity in Hill's frame vs time.

Table 1 Nonlinear model solution with RHC, case 1: cost values and final states for different controllers

	J	$r_x(T)$, m	$r_y(T)$, m	$r_z(T)$, m	$v_x(T)$, m/s	$v_y(T)$, m/s	$v_z(T)$, m/s
$\tilde{d}_{\text{pwlin}}$	0.16	−0.24	−29.9	−0.5	-3×10^{-3}	-3×10^{-3}	-9×10^{-3}
$\tilde{d}_{\text{pwconst}}$	4.26	−0.87	−31.2	−2.8	-23×10^{-3}	-40×10^{-3}	-77×10^{-3}
$\tilde{d}\equiv 0_{2n\times1}$	2246	−66.5	−20.5	8.5	−1.3	0.23	0.15

Table 2 Nonlinear model solution with RHC, case 2: cost values and final states for different controllers

	J	$r_x(T)$, m	$r_y(T)$, m	$r_z(T)$, m	$v_x(T)$, m/s	$v_y(T)$, m/s	$v_z(T)$, m/s
$\tilde{d}_{\text{pwlin}}$	0.42	0.6	−53.6	0.67	-6×10^{-3}	-9×10^{-3}	10×10^{-3}
$\tilde{d}_{\text{pwconst}}$	2.28	0.21	−55.3	2.1	-18×10^{-3}	-60×10^{-3}	54×10^{-3}
$\tilde{d}\equiv 0_{2n\times1}$	921.1	−42.8	−47	−2.5	−0.88	0.14	-38×10^{-3}

and control sequences is performed substantially faster, on the order of milliseconds.

In contrast, when the actual d rather than its approximation is used, the TPBVP solution is obtained numerically using *ode45* and *fsolve* in MATLAB. Although the computation time is affected by the initial guess of ψ_0, for $\Delta t = 100$ s, default solver settings, and an initial guess of $\psi_0 = 0_{6\times1}$, the computation time is about 7.8 s for test case 1 and 9.3 s for test case 2. For poor initial guesses of ψ_0, computation times are higher.

C. Nonlinear Model Results

We use a RHC implementation of the proposed approach to control the nonlinear spacecraft model. The sampling time is set to $\Delta t = 100$ s and, based on the current state, we recompute the solution to the TPBVP at every sampling instant t_k, $k = 1, 2, \ldots, \nu - 1$, for a receding and shrinking time horizon $T - t_k$. The controls $u_{\text{pwlin}}(t_k)$ and $u_{\text{pwlin}}(t_{k+1})$ are computed according to Eq. (17), and we apply the control

$$u_{\text{interp}}(t) = u_{\text{pwlin}}(t_k) + (u_{\text{pwlin}}(t_{k+1}) - u_{\text{pwlin}}(t_k))(t - t_k)/\Delta t$$

to the spacecraft during the sampling interval $t \in [t_k, t_{k+1})$. This receding horizon implementation provides a form of feedback to compensate for unmodeled effects not present in the linear model. Although the respective matrices in Eqs. (11) and (20) are built offline before the maneuver (computation times with $\Delta t = 100$ s: ≈0.3 s for case 1 and ≈0.4 s for case 2; see top plot in Fig. 2), the computation times for recomputing the control are negligible. For recomputing the control according to the proposed RHC scheme, we record a maximum total computation time over all sampling instants of 1.5 ms for case 1 and 1.8 ms for case 2, where the average total computation time over all sampling instants is about 1 ms for both cases. Hence, the RHC implementation is suitable for real-time applications. Note that it is not necessary to recompute the disturbance term $d(t)$, because the nominal trajectory given by the target orbit does not change.

Figures 3–5 show the control input accelerations as well as the spacecraft's position and velocity relative to the target orbit for cases 1 and 2, defined in Sec. IV.A using the proposed RHC implementation. In both cases, the controller is able to drive the spacecraft to the desired target orbit.

The cost values for the trajectories in Figs. 3–5 are listed in Tables 1 and 2, which also include the final states. In addition to the RHC scheme based on the piecewise-linear approximation of d ($\tilde{d}_{\text{pwlin}}$), Tables 1 and 2 include the results when using the RHC scheme with either a piecewise-constant approximation of d [i.e., $\tilde{d}_{\text{pwconst}}(t) = [d^T(t_k), 0_{1\times n}]^T$ for $t \in [t_k, t_{k+1})$] or without taking into account the disturbance when computing the control ($\tilde{d} \equiv 0_{2n\times1}$).

It is evident that taking into account the disturbance for the control improves the performance because the controller with $\tilde{d} \equiv 0_{2n\times1}$ performs poorly compared to the controllers based on $\tilde{d}_{\text{pwlin}}$ and $\tilde{d}_{\text{pwconst}}$. Moreover, the piecewise-linear approximation of d improves the performance compared to a piecewise-constant approximation, where the advantage of using $\tilde{d}_{\text{pwlin}}$ increases with increasing Δt. Note that the weight for $r_y(T)$ (final position on the target orbit) is smaller compared to the terminal weights on the other states, which explains the deviations compared to the other states in Tables 1 and 2.

V. Conclusions

A linear quadratic optimal control problem was considered for linear systems with a previewed time-varying disturbance term $d(t)$. A closed-form solution was derived based on Pontryagin's maximum principle by approximating $d(t)$ by a piecewise-linear function of time using equidistant time intervals. It was shown that the error due to the piecewise-linear approximation can be bounded by a quadratic function of the length of the time intervals. The closed-form solution can readily be implemented in computer code and allows for fast computations in real time. Besides, the proposed approach can be used to warm start nonlinear optimal control solvers that require a good initial guess for convergence and can, in addition, handle state and control constraints. The approach was applied to spacecraft orbital maneuvering, where disturbances due to atmospheric drag and J_2 and J_3 perturbation were taken into account. Two test cases with different initial conditions and circular target orbits were treated. In both cases, the spacecraft was successfully driven to the prescribed target orbit using a receding horizon control implementation of the closed-form solution to the LQ problem.

Acknowledgment

This research is supported by the National Science Foundation Award, number EECS 1404814.

References

[1] Tsuchiya, T., Shinada, K., Abe, S., and Egami, T., "Robot Trajectory Control by Preview Control and Adaptive Control," *Proceedings of the IEEE Workshop on Intelligent Robots*, IEEE, Piscataway, NJ, Oct. 1988, pp. 125–130.

[2] Kajita, S., Kanehiro, F., Kaneko, K., Fujiwara, K., Harada, K., Yokoi, K., and Hirukawa, H., "Biped Walking Pattern Generation by Using Preview Control of Zero-Moment Point," *IEEE International Conference on Robotics and Automation, Proceedings (ICRA'03)*, Vol. 2, IEEE, Piscataway, NJ, 2003, pp. 1620–1626.

[3] Takaba, K., "A Tutorial on Preview Control Systems," *SICE 2003 Annual Conference*, Vol. 2, IEEE, Piscataway, NJ, 2003, pp. 1388–1393.

[4] Bruyne, S. D., der Auweraer, H. V., Anthonis, J., Desmet, W., and Swevers, J., "Preview Control of a Constrained Hydraulic Active Suspension System," *Proceedings of the IEEE Conference on Decision and Control*, IEEE, Piscataway, NJ, Dec. 2012, pp. 4400–4405.

[5] Zhaojian, L., Kolmanovsky, I., Atkins, E., and Jianbo, L., "Cloud Aided Semi-Active Suspension Control," *Proceedings of the 2014 IEEE Symposium on Computational Intelligence in Vehicles and*

Transportation Systems (CIVTS), IEEE, Piscataway, NJ, Dec. 2014, pp. 76–83.

[6] Birla, N., and Swarup, A., "Optimal Preview Control: A Review," *Optimal Control Applications and Methods*, Vol. 36, No. 2, 2015, pp. 241–268. doi:10.1002/oca.v36.2

[7] Kanzaki, S., Okada, K., and Inaba, M., "Bracing Behavior in Humanoid Through Preview Control of Impact Disturbance," *5th IEEE-RAS International Conference on Humanoid Robots*, IEEE, Piscataway, NJ, 2005, pp. 301–305.

[8] Farooq, A., and Limebeer, D. J., "Path Following of Optimal Trajectories Using Preview Control," *Proceedings of the 44th IEEE Conference on Decision and Control*, IEEE, Piscataway, NJ, 2005, pp. 2787–2792.

[9] Negm, M. M., Bakhashwain, J. M., and Shwehdi, M., "Speed Control of a Three-Phase Induction Motor Based on Robust Optimal Preview Control Theory," *IEEE Transactions on Energy Conversion*, Vol. 21, No. 1, 2006, pp. 77–84. doi:10.1109/TEC.2005.858072

[10] Shimmyo, S., Sato, T., and Ohnishi, K., "Biped Walking Pattern Generation by Using Preview Control Based on Three-Mass Model," *IEEE Transactions on Industrial Electronics*, Vol. 60, No. 11, 2013, pp. 5137–5147. doi:10.1109/TIE.2012.2221111

[11] Moran, A., Mikami, Y., and Hayase, M., "Analysis and Design of H_∞ Preview Tracking Control Systems," *4th International Workshop on Advanced Motion Control, AMC'96-MIE Proceedings*, Vol. 2, IEEE, Piscataway, NJ, 1996, pp. 482–487.

[12] Mianzo, L., and Peng, H., "A Unified Framework for LQ and H_∞ Preview Control Algorithms," *Proceedings of the IEEE Conference on Decision and Control*, IEEE, Piscataway, NJ, Dec. 1998, pp. 2816–2821.

[13] Mehra, R. K., Amin, J. N., Hedrick, K. J., Osorio, C., and Gopalasamy, S., "Active Suspension Using Preview Information and Model Predictive Control," *Proceedings of the 1997 IEEE International Conference on Control Applications*, IEEE, Piscataway, NJ, 1997, pp. 860–865.

[14] Cole, D., Pick, A., and Odhams, A., "Predictive and Linear Quadratic Methods for Potential Application to Modelling Driver Steering Control," *Vehicle System Dynamics*, Vol. 44, No. 3, 2006, pp. 259–284. doi:10.1080/00423110500260159

[15] Laks, J., Pao, L. Y., Simley, E., Wright, A., Kelley, N., and Jonkman, B., "Model Predictive Control Using Preview Measurements from Lidar," *49th AIAA Aerospace Sciences Meeting*, AIAA Paper 2011-0813, 2011.

[16] Spencer, M. D., Stol, K. A., Unsworth, C. P., Cater, J. E., and Norris, S. E., "Model Predictive Control of a Wind Turbine Using Short-Term Wind Field Predictions," *Wind Energy*, Vol. 16, No. 3, 2013, pp. 417–434. doi:10.1002/we.v16.3

[17] Calafiore, G. C., and Fagiano, L., "Robust Model Predictive Control via Scenario Optimization," *IEEE Transactions on Automatic Control*, Vol. 58, No. 1, 2013, pp. 219–224. doi:10.1109/TAC.2012.2203054

[18] Zidek, R. A. E., and Kolmanovsky, I. V., "Approximate Optimal Control of Nonlinear Systems with Quadratic Performance Criteria," *American Control Conference (ACC)*, IEEE, Piscataway, NJ, 2015, pp. 5587–5592.

[19] Bernstein, D. S., *Matrix Mathematics*, Princeton Univ. Press, Princeton, NJ, 2009, p. 598, Chap. 6.

[20] Khalil, H. K., *Nonlinear Systems*, 3rd ed., Prentice–Hall, Upper Saddle River, NJ, 2002, pp. 651–652.

[21] Picone, J. M., Hedin, A. E., Drob, D. P., and Aikin, A. C., "Empirical Model of the Atmosphere: Statistical Comparisons and Scientific Issues," *Journal of Geophysical Research*, Vol. 107, No. 15, 2002, pp. 1–16.

[22] Bate, R. B. D., Mueller, D., and White, J. E., *Fundamentals of Astrodynamics*, Dover, New York, 1971, Chap. 9.7.

[23] Longuski, J. M., Guzman, J. J., and Prussing, J. E., *Optimal Control with Aerospace Applications*, Springer, New York, 2014, pp. 204–205.

[24] Wie, B., *Space Vehicle Dynamics and Control*, AIAA, Reston, VA, 2008, pp. 110, 299–300.